

Development of Chitosan-Based Hydrogel Containing Polyvinyl Alcohol, Cellulose, and ZnO Nanoparticles for Potential Biomedical Applications

Suman Dewanjee¹, Hasan Ahmed², Mohammad Ali Tanvir³, Muttakee Bin Ali¹, Safia Aktar Dipa⁴, and Md. Ibrahim Al Imran^{1,*}

¹*Department of Biomedical Physics & Technology, University of Dhaka, Dhaka-1000, Bangladesh*

²*Department of Leather Engineering, Khulna University of Engineering and Technology, Khulna-9203, Bangladesh.*

³*Department of Biomedical Engineering, Bangladesh University of Engineering and Technology, Dhaka- 1000, Bangladesh.*

⁴*Department of Electrical and Electronic Engineering, Bangabandhu Sheikh Mujibur Rahman Science and Technology University, Gopalganj -8100., Bangladesh.*

(Received: 18 August 2024 ; Accepted: 19 December 2024)

Abstract

Waste materials such as chitosan-rich shrimp shells and cellulose-containing sugarcane bagasse are discarded in substantial quantities worldwide. These by-products hold untapped potential for creating sustainable biomaterials, such as hydrogels, for biomedical applications. This research bridges sustainable development and biomedical engineering by producing a biocompatible, thermally stable, mechanically optimized, and infection-resistant hydrogel. The study examines a composite hydrogel formulated from chitosan, polyvinyl alcohol (PVA), Tannic acid (TA), and zinc oxide nanoparticles (ZnONP), with glutaraldehyde and gelatin powder as a cross-linking agent. Glutaraldehyde enhances cross-linking with chitosan's amine groups, improving the hydrogel's thermal stability, while ZnONP functionalization enhances its antibacterial properties. Comprehensive evaluations covered structural integrity, cell viability, swelling ratio, water vapor transmission rate, pore size, and mechanical and thermal properties. Analytical techniques such as FTIR and XRD confirmed favorable swelling ratios, porosity, and water vapor permeability, highlighting the hydrogel's suitability for wound dressings. By achieving optimal degrees of swelling (DSR) and water vapor transmission rates (WVTR), the chitosan-based PVA/cellulose/ZnONP hydrogel demonstrates promise for advanced wound healing applications, supporting both skin restoration and infection control. The novelty lies in the way of approach to bring sustainability and biomedical engineering together.

Keywords: Hydrogel, Chitosan, Tannic acid, ZnO nanoparticles, Cellulose fiber.

I. Introduction

To address the high demand for sustainable materials, this research focuses on developing a chitosan-based hydrogel from recyclable, natural materials, specifically chitosan derived from shrimp shells and cellulose from sugarcane bagasse. The primary goal is to bridge the gap between sustainability and biomedical applications, contributing to environmental preservation and potential advancements in wound care. Wound healing is a complex physiological process involving a sequence of cellular events to repair damaged tissue¹. In recent years, hydrogels have emerged as promising candidates for wound dressings due to their high biocompatibility, moisture retention, and capacity to maintain a conducive environment for wound healing². Among these, chitosan-based hydrogels are particularly notable for their biodegradability, biocompatibility, and inherent antibacterial activity, properties that make them especially suited for chronic wound care^{3,4}. Natural antibacterial effect of chitosan, derived from its polycationic structure, can help to prevent and control infections at the wound site⁵. To further enhance the functionality of chitosan hydrogels, researchers have explored involving additional components such as polyvinyl

alcohol (PVA) and cellulose, which improve mechanical strength, water absorption, and durability⁶.

Tannic acid (TA), a special kind of polyphenol, has cyclic glucose and five digalloyl groups^{7,8}. TA possesses weak acidity because of its large number of phenolic hydroxyl groups and it ionizes at a pH value higher than 4.5, and it will possess negative charges in an aqueous solution after ionization^{9,10}. TA can be considered a good modifier to improve the surface properties because it is negatively charged in solution and has high adhesiveness on various nonporous or porous substrates¹¹⁻¹³. So, TA addition does improve the quality of biomaterials in general.

A key advancement in hydrogel formulation involves the addition of ZnONPs, known for their potent antibacterial activity and ability to stimulate tissue regeneration. ZnONPs have shown effectiveness against a broad spectrum of bacterial pathogens, making them ideal for wound care applications, where infection control is critical^{14,15}.

An ideal hydrogel's biocompatibility, coupled with its tunable porosity, makes it applicable for tissue engineering

*Author for correspondence. e-mail: imran.bmpt@du.ac.bd

scaffolds, offering a conducive environment for cell growth and differentiation. Its potential as a burn treatment dressing is significant, as it helps to prevent infection, promotes healing, and maintains a moist environment that facilitates skin regeneration¹⁶. The hydrogel's controlled swelling and degradation properties can be tailored to enable the gradual release of therapeutic agents, positioning it as a potential drug delivery system¹⁷. Additionally, the incorporation of ZnO nanoparticles imparts strong antibacterial properties, enhancing its efficacy as a coating material and enabling it to degrade organic pollutants^{18,19}. Its excellent fluid absorption capacity, combined with its inherent antibacterial activity, further supports its application in surgical settings²⁰. Therefore, the hydrogel can function as a hemostatic agent or surgical sponge, controlling bleeding during procedures while minimizing the risk of infection.

By developing a composite hydrogel with chitosan, PVA, cellulose, and ZnONPs, this study aims to create a material that not only enhances wound healing but also promotes tissue regeneration and prevents bacterial colonization. This study focuses on the synthesis and characterization of a chitosan-based antibacterial hydrogel containing PVA, cellulose, and ZnO nanoparticles, targeting enhanced performance in wound dressing applications²¹. The hydrogel synthesis will involve a crosslinking process using glutaraldehyde to achieve a robust, interconnected network⁴. PVA and cellulose are expected to enhance mechanical properties, flexibility, and water retention, while ZnONP is included to confer antibacterial efficacy against both gram-positive and gram-negative bacteria²². We have conducted characterization tests comprehensively to assess the hydrogel's physicochemical properties, including swelling behavior, porosity, mechanical strength, and degradation profile using analytical techniques such as scanning electron microscopy (SEM), Fourier-transform infrared spectroscopy (FTIR), and X-ray diffraction (XRD). Additionally, cytocompatibility will be assessed using cell viability assays to ensure biocompatibility and non-toxicity.

II. Methodology

Chitosan extraction

Demineralizing, deproteinizing, and deacetylating processes were used to create chitosan from prawn shells. At first, the collected shells were cleaned with acetic vinegar for 30 minutes, followed by 72 hours of sun drying. Calcium carbonate and calcium chloride were removed by agitation for 8 hours at 400°C, followed by sun-drying for 72 hours. After that, the components passed through filtration to get a neutral pH and were dried in an oven. Afterward, all organic components, including proteins, were removed. Alkali solution, commonly 10% w/w aqueous sodium hydroxide (NaOH) was heated to 60°C for 3 hours and washed with deionized water to eliminate extra NaOH. The finished product was then dried in the sun for three days. The decolorization process was then performed by stirring 8% HCl with 2% KMnO₄ at 600°C for 30 minutes. After being

dried in the sun for 96 hours, the substance obtained was pure chitin. In the final step, acetyl groups were removed from chitin and finalized into chitosan by heating while exposed to a concentrated alkali solution, such as sodium hydroxide (NaOH) or potassium hydroxide (KOH). Utilizing alkali solutions, the process was carried out at 700°C for 4 hours with concentrations starting at 50% w/w. Finally, to reach a neutral state, the material was repeatedly washed with distilled water and dried under the sun for 48 hours.

Cellulose fiber extraction

Initially, sugarcane fiber was collected and sorted, then rinsed with distilled water and dried for 12 hours at 60°C, then washed with 80% alcohol. After being sieved into several mesh sizes, the dried sugarcane fiber was finely mashed in a commercial blender. Sugarcane bagasse was washed to remove sugar and other contaminants. The bagasse was repeatedly rinsed in water until the color of water was observed. The sugarcane bagasse fibers were sieved to remove the powder after being exposed to the sun for two days (about 22 hours). After sifting 300g of fibers, 5 L of a 5 wt% NaOH solution was poured over the material. The second container held 5 L of diluted acetic acid solution (10 wt% of the concentrated solution) and 10 L of distilled water. The suspension was stirred every five to ten minutes throughout the hour-long therapy. Acetic acid solution was used to soak the fibers for 10 minutes after separation. The neutralized fibers were then rinsed several times under running water before being put in a container with distilled water. Fibers were created for initial investigation in a similar manner, albeit with different concentrations and less NaOH. Finally, fibers were synthesized by heating with ethanol for 6 hours at 40°C with continuous stirring and after that, fibers were exposed to the sun for 16 hours.

Hydrogel fabrication

To begin with, the cellulose powder was immersed in distilled water, then tannic acid at 10% was added and carried out at 60°C for three hours at 300 rpm. The resulting powder was then filtered and put through 4 days of dialysis using a dialysis bag. It was then freeze-dried and kept for later use in a freezer at 24°C. PVA was dissolved in distilled water (DW) at 80°C to 85°C to produce 10% solution, with a ratio of 1:4 between PVA and gelatin. Chitosan powder was immersed in 1% acetic acid to create chitosan solutions. DW was used to dissolve the 20% gelatin, and ZnONP was created by dissolving the gelatin in distilled water and stirring. Tannic acid was combined with sugarcane fiber powder and stirred while the ratio for the sample of SF: TA was 1.55:1. Gel was prepared by combining PVA and chitosan (1:5.67) solutions at room temperature and found long-lasting gel formation as well as would no distortion. After that, according to Fig. 1 and Table 1, the defined weight ratios of glutaraldehyde (glu) (aq) and HCl(aq) were dissolved in acetone and mixed with gels at 40°C for an hour and five different hydrogels (H1, H2, H3, H4, and H5) were created by following the order and data. Finally, hydrogels were fabricated by freezing and

thawing the solution four times (8 hours at -20°C ; 3 hours at room temperature). Hydrogels were considered clean once

their pH was lowered to 7.0 through repeated washings with distilled water.

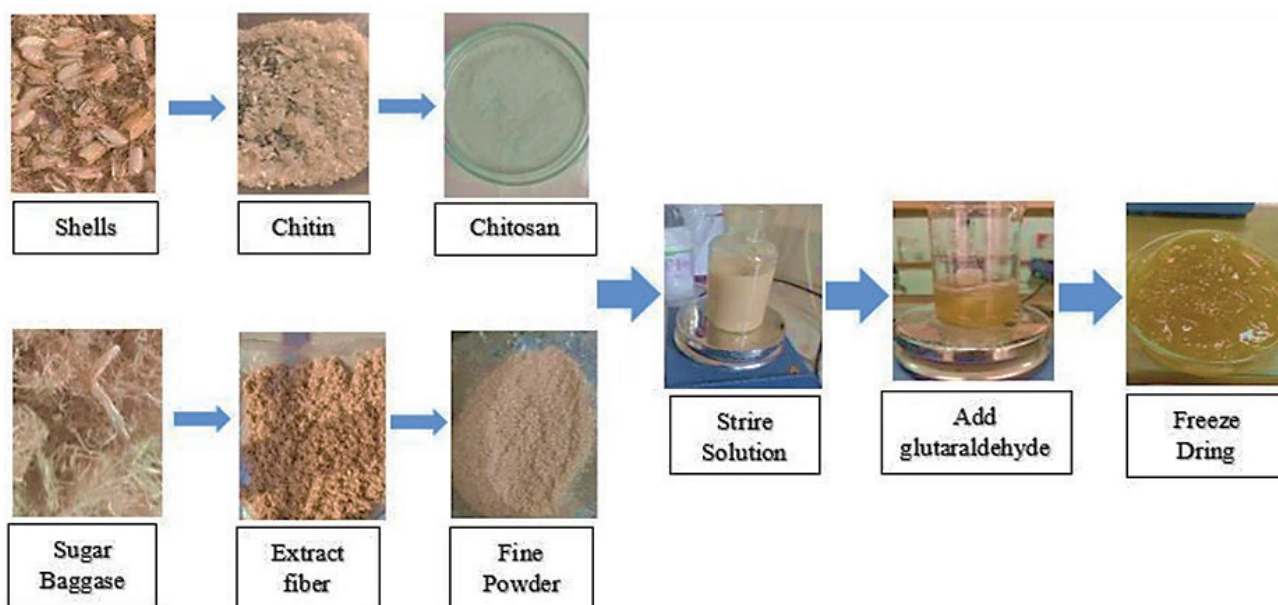


Fig. 1. Synthesis of hydrogel

Table 1. Weight percentage (%Wt) for preparation of hydrogels

Sample Name	PVA-Gelatin (%wt)	PVA-CS (%wt)	SF-TA (%wt)	ZnONP (%wt)	Glu-Ace-tone-HCL(%wt)	DW(%wt)
H1	80	0	0	0.5	2	17.5
H2	20	60	2	0.2	1.8	16
H3	30	50	1	0.1	1.5	16.5
H4	40	40	2	0.3	1	16.7
H5	0	80	0	0.4	2	17.6

III. Results

FTIR

FTIR spectroscopy divides the spectrum into two primary regions: the functional group region ($4000\text{--}1500\text{ cm}^{-1}$) and the fingerprint region ($1500\text{--}400\text{ cm}^{-1}$). The functional group region displays characteristic absorption bands associated with distinct functional groups (e.g., O–H, N–H, C=O), making it useful for identifying molecular components. Meanwhile, the fingerprint region contains complex patterns unique to each compound, serving as a molecular “fingerprint” that enables precise identification of materials. The FTIR spectrum in the synthesized chitosan-based hydrogel reveals several peaks that elucidate its molecular structure and interactions. A broad absorption peak observed at 3358 cm^{-1} in the functional group region corresponds to the O–H stretching vibrations of polyvinyl alcohol and the N–H stretching from chitosan, indicating extensive hydrogen bonding within the hydrogel matrix^{23,24}. This broad peak reflects the combined hydroxyl and amine groups of PVA, cellulose, and chitosan

and the enhanced hydrogen-bonding interactions due to the matrix structure. The presence of ZnO nanoparticles, which are incorporated for their antibacterial properties, contributes to smoothing effects on the peaks in the $1100\text{--}1200\text{ cm}^{-1}$ range, suggesting an interaction with the hydrogel matrix that reduces distinct absorption bands seen in pure PVA and chitosan^{23,25}. A distinct peak at 1641 cm^{-1} is attributed to the amide I band, associated with the C=O stretching in chitosan’s N–H linkage, reinforcing the presence of chitosan as a core component in the hydrogel matrix²⁶. Additionally, cross-linking among cellulose, chitosan, and PVA shifts their peaks into a broad absorption band across the $3000\text{--}3800\text{ cm}^{-1}$ range, further confirming hydrogen-bonding interactions that stabilize the biocomposite structure²⁷. Other significant peaks in the functional group region provide further insight into the material’s composition. For example, the peak at 1274 cm^{-1} , indicative of C–O stretching vibrations, is characteristic of polysaccharides and likely represents either cellulose or chitosan. The slight shift of the peak in the hydrogel matrix suggests modifications due to the cross-linked structure²⁸.

At 1373 cm^{-1} , CH_3 bending vibrations are observed, typical of acetylated units in chitosan, with possible overlapping contributions from C–H bending in PVA²⁴. The 1431 cm^{-1} peak corresponds to C–N stretching, which signifies the

presence of primary amine groups in chitosan, while the 1544 cm^{-1} peak is associated with N–H bending vibrations, confirming integration of chitosan within the matrix. Fig. 2(a) shows the FTIR patterns of novel hydrogel.

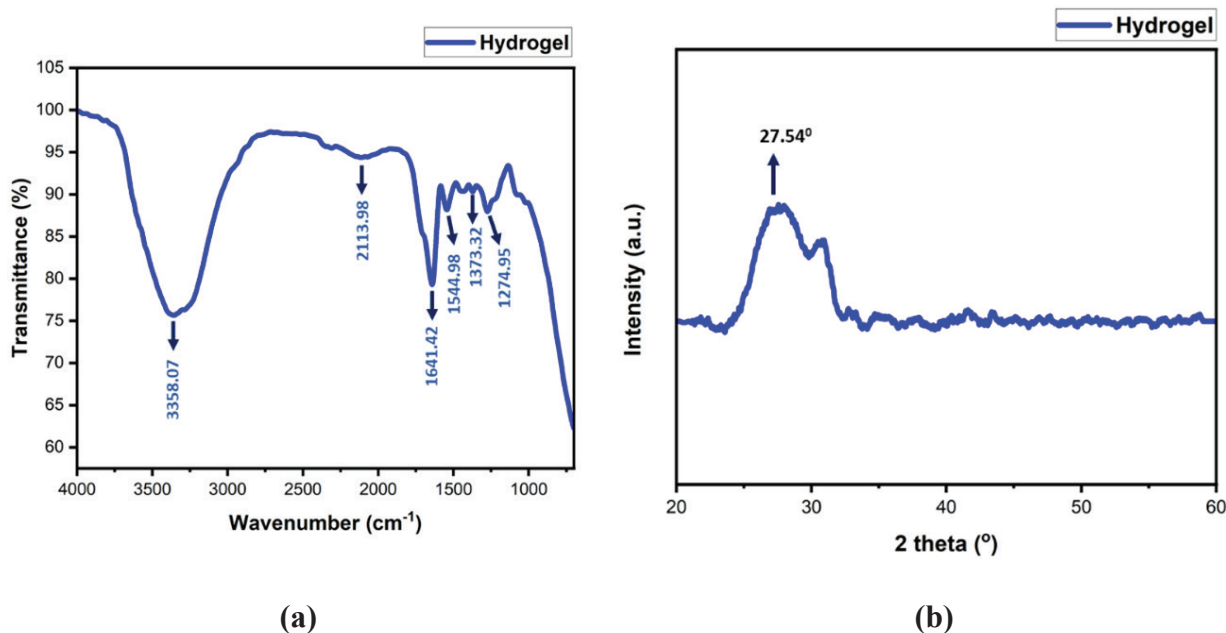


Fig. 2. (a)FTIR and (b)XRD graphs of the hydrogel

XRD

Fig. 2(b) shows the XRD patterns of novel hydrogel. We can see from the figure that the strongest diffraction peak of both is around $25\text{--}33^\circ$ due to the amorphous structure, indicating that the crystalline nature of the PVA, chitosan, and cellulose individually has not changed after it is transformed into the hydrogel. Characteristic peaks of ZnONP are not observed in hydrogel spectra the reason of which may be the slight presence of ZnONP in hydrogel structure²³.

Gel content

The gel content of hydrogels, indicating crosslinked polymer chains, is influenced by interactions among the components. Increasing the PVA ratio in the hydrogel structure results in higher gel content, indicating more crosslinking and a denser network. Conversely, increasing the chitosan ratio decreases gel content due to interference with PVA cross-linking. The interaction between PVA and other components is significant in determining crosslinking, providing control over strength and flexibility. The gel content is sensitive to the amount of ZnONP added, with an optimum of 1% weight. Increased ZnONP enhances interaction with polymer chains, raising the gel content. Similar effects are observed with other nanoparticles. The number of freeze-thaw cycles also impacts gel content by promoting hydrogel structure formation and increased interaction between components. Understanding and controlling these factors are vital for tailoring hydrogel properties for biomedical applications.

Water Vapor Transmission Rate (WVTR)

This test is crucial for wound healing, with ideal values ranging from 2000 to 2500 $\text{g/m}^2\text{day}$. Normal skin, first-degree burns, and granulating wounds have WVTR values of 200, 300, and 5000 $\text{g/m}^2\text{day}$, respectively. High WVTR can lead to scarring, while low WVTR causes exudates and bacterial growth. In hydrogel systems, WVTR falls within the 2200–4550 $\text{g/m}^2\text{day}$ range. Adding PVA hinders water vapor passage, and increased freeze-thaw cycles enhance crystallinity, reducing WVTR. These hydrogel systems can be considered ideal wound dressings, comparable to commercial samples.

Porosity test

Porosity testing is necessary for hydrogels to assess their pore structure and determine their ability to absorb and release fluids, which is important for wound healing applications. The porosity of the control hydrogel was found to be 49.43%, which decreased to values ranging from 31.67% to 41.24% with the incorporation of different materials. The reduction of porosity in the hydrogels was attributed to factors such as incorporating cellulose, chitosan, Tannic acid, and ZnONPs. Higher concentrations of chitosan resulted in lower porosity, with the lowest porosity of 31.67% observed in the hydrogel formulation with dense chitosan and gelatin incorporation. This porosity reduction indicates improved structural integrity and potential for controlled fluid absorption and release in the hydrogel dressings.

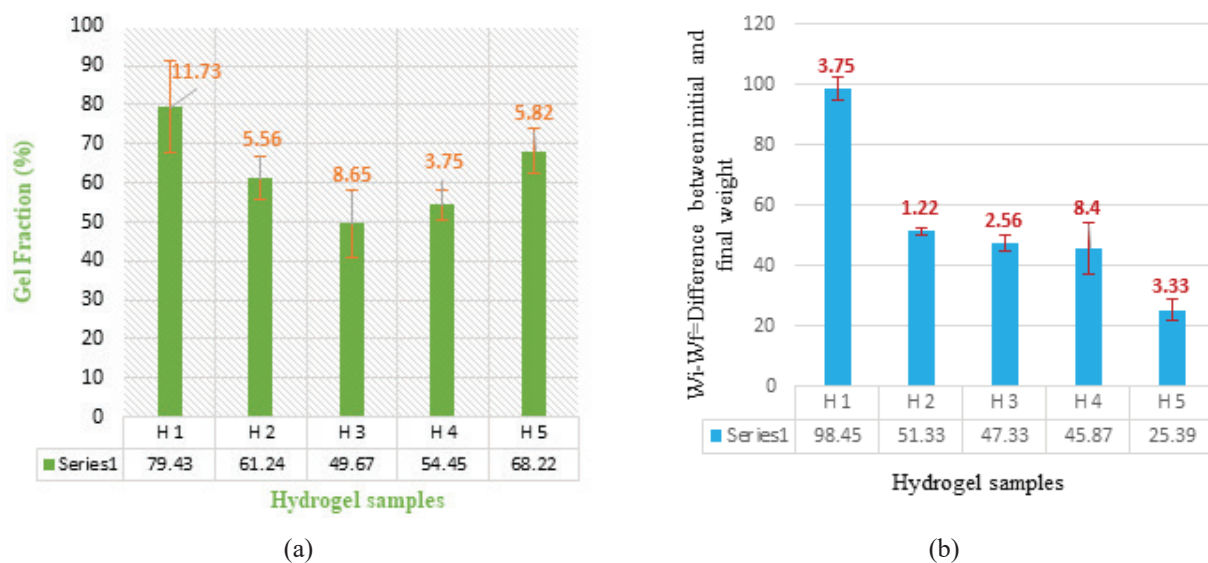


Fig. 3. (a) Gel fraction analysis and (b) Water vapor permeability test

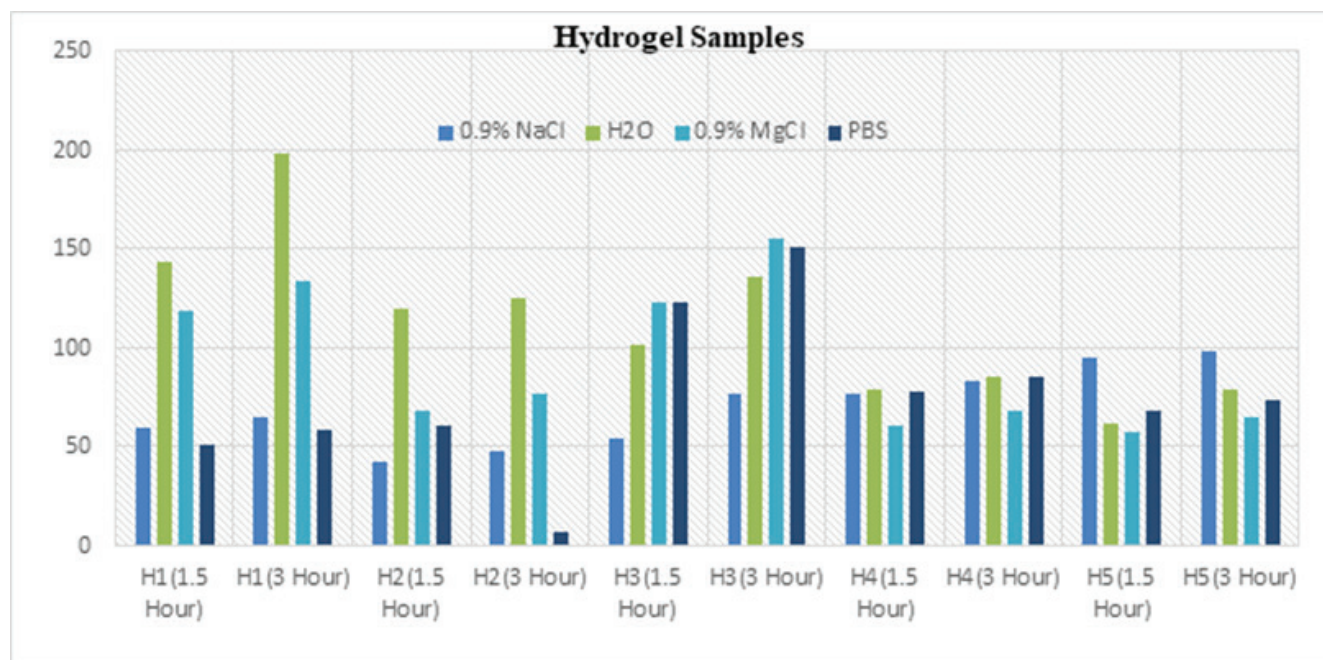


Fig. 4. Results of swelling test

Table 2. Numerical data of swelling test

Sample (Hour)	H1(1.5)	H1(3)	H2(1.5)	H2(3)	H3(1.5)	H3(3)	H4(1.5)	H4(3)	H5(1.5)	H5(3)
0.9% NaCl	59.44	65.44	41.98	48.12	54.56	76.56	76.56	83.44	94.67	97.96
H ₂ O	143.39	198.34	119.36	125.34	101.12	136.34	79.3	85.67	62.18	79.44
0.9% MgCl	119.22	134.33	68.44	76.44	123.11	155.45	60.44	68.49	57.33	65.33
PBS	51.33	58.66	61.23	7.44	123.22	151.33	78.33	85.33	68.22	73.67

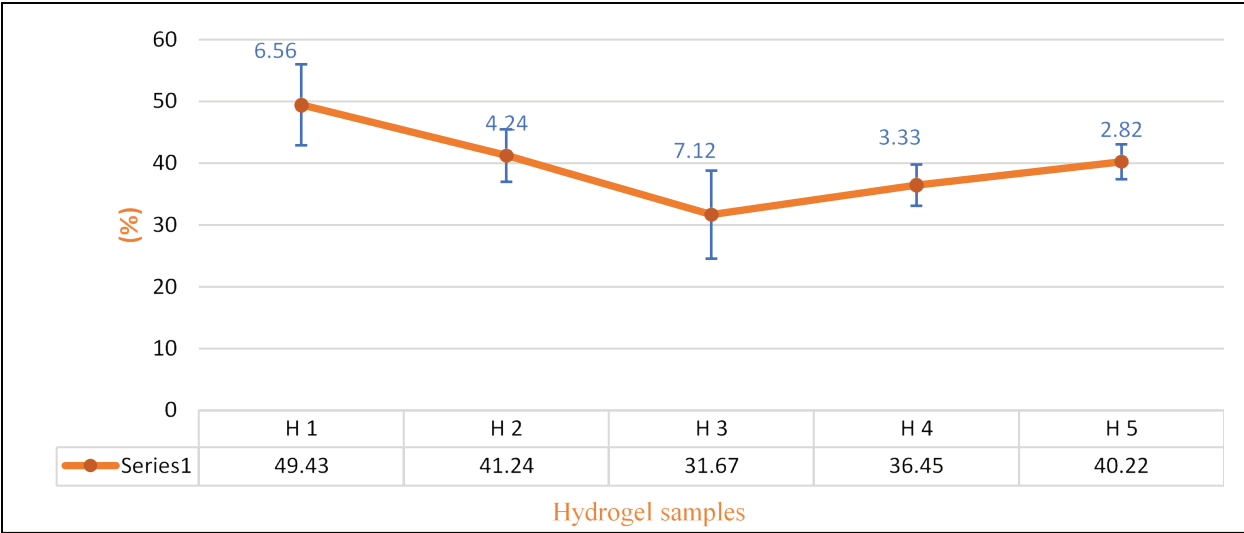


Fig. 4. Illustration of porosity test

IV. Discussion and Conclusion

In this study, the investigation and characterization of PVA/CS/TA coated SF hydrogels with the inclusion of ZnONP for potential application as wound dressings are discussed. The hydrogel composition, ranging from 50% to 80% gel, exhibited an increased swelling ratio with higher ZnONP concentration, indicating its ability to absorb body fluids. The hydrogel demonstrated antibacterial activity against both gram-positive and gram-negative bacteria and possessed a porosity of 31.67%, suggesting its potential for fluid absorption. The addition of SF improved the hydrogel's crystallinity, while the incorporation of ZnONP enhanced its antibacterial. Tannic acid contributed to skin regeneration, glutaraldehyde promoted gel formation, gelatin facilitated crosslinking, and PVA improved the solubility of chitosan.

The hydrogel also exhibited excellent wound fluid absorption rates, particularly after 48 hours. Furthermore, tannic acid further enhanced the mechanical properties of the hydrogel, making it well-suited for wound healing. With concentration-dependent improvements in antibacterial, antioxidant, and adhesiveness capabilities, the biodegradable, biocompatible, and non-toxic nature of chitosan makes it an attractive choice for medical applications. Further, in vivo experiments are necessary to validate the clinical potential of these hydrogels in facilitating wound healing. The novelty of this research lies in its innovative approach to seamlessly integrate sustainability with biomedical engineering. By utilizing abundant waste materials such as chitosan-rich shrimp shells and cellulose-containing sugarcane bagasse, this study creates a sustainable biomaterial with significant potential for biomedical applications. This novel strategy not only addresses environmental concerns but also advances the development of biocompatible, thermally stable, and mechanically optimized hydrogels for use in wound healing, highlighting the synergistic benefits of sustainable practices and cutting-edge biomedical engineering.

References

1. García-Hernández, A. B., E. Morales-Sánchez, B. M. Berdeja-Martínez, M. Escamilla-García, M. P. Salgado-Cruz, M. Rentería-Ortega, R. R. Farrera-Rebollo, M. A. Vega-Cuellar, and G. Calderón-Domínguez. 2022. PVA-based electrospunbiomembranes with hydrolyzed collagen and ethanolic extract of *Hypericum perforatum* for potential use as wound dressing: Fabrication and characterization. *Polymers (Basel)*, **14**, 1981.
2. Ramphul, H., A. Bhaw-Luximon, and D. Jhurry. 2017. Sugarcane bagasse derived cellulose enhances performance of polylactide and polydioxanoneelectrospun scaffold for tissue engineering. *Carbohydrate Polymers*, **178**, 238–250.
3. Elangwe, C. N., S. N. Morozkina, R. O. Olekhovich, A. Krasichkov, V. O. Polyakova, and M. V. Uspenskaya. 2022. A review on chitosan and cellulose hydrogels for wound dressings. *Polymers (Basel)*, **14**, 5163.
4. El Knidri, H., R. Belaabed, A. Addaou, A. Laajeb, and A. Lahsini. 2018. Extraction, chemical modification and characterization of chitin and chitosan. *International Journal of Biological Macromolecules*, **120**, 1181–1189.
5. Joorabloo, A., M. T. Khorasani, H. Adeli, Z. Mansoori-Moghadam, and A. Moghaddam. 2019. Fabrication of heparinized nanoZnO/poly(vinylalcohol)/carboxymethyl cellulose bionanocomposite hydrogels using artificial neural network for wound dressing application. *Journal of Industrial and Engineering Chemistry*, **70**, 253–263.
6. Darling, N. J., E. Sideris, N. Hamada, S. T. Carmichael, and T. Segura. 2018. Injectable and spatially patterned microporous annealed particle (MAP) hydrogels for tissue repair applications. *Advanced Science*, **5**, 1801046.
7. Kim, B. J., J. K. Lee, and I. S. Choi. 2019. Iron gall ink revisited: Hierarchical formation of Fe(III)–tannic acid coacervate particles in microdroplets for protein condensation. *Chemical Communications*, **55**, 2142–2145.
8. Xu, W., E. H. Han, and Z. Wang. 2019. Effect of tannic acid on corrosion behavior of carbon steel in NaCl solution. *Journal of Materials Science & Technology*, **35**, 64–75.

9. Luo, R., W. Zhang, X. Zhou, and H. Ji. 2017. Tannic acid as a polyphenol material-assisted synthesis of cyclic carbonates using CO₂ as a feedstock: Kinetic characteristic and mechanism studies. *Chinese Journal of Chemistry*, **35**, 659–664.
10. Asadi, N., H. Pazoki-Toroudi, A. R. Del Bakhshayesh, A. Akbarzadeh, S. Davaran, and N. Annabi. 2021. Multifunctional hydrogels for wound healing: Special focus on biomacromolecular based hydrogels. *International Journal of Biological Macromolecules*, **170**, 728–750.
11. Silva, L. N., K. R. Zimmer, A. J. Macedo, and D. S. Trentin. 2016. Plant natural products targeting bacterial virulence factors. *Chemical Reviews*, **116**, 9162–9236.
12. Sun, W., Y. Zhao, J. Zhou, X. Cheng, J. H. He, & J. M. Lu. 2019. One-Step fabrication of bio-compatible coordination complex film on diverse substrates for ternary flexible memory. *Chemistry—A European Journal*, **25**, 4808–4813.
13. Zhang, A., Y. Liu, D. Qin, M. Sun, T. Wang, & X. Chen. 2020. Research status of self-healing hydrogel for wound management: A review. *International Journal of Biological Macromolecules*, **164**, 2108–2123.
14. Perumal, G., S. Pappuru, D. Chakraborty, A. M. Nandkumar, D. K. Chand, & M. Doble. 2017. Synthesis and characterization of curcumin loaded PLA—Hyperbranched polyglycerol electrospun blend for wound dressing applications. *Materials Science and Engineering: C*, **76**, 1196–1204.
15. Beylergil, B., M. Tanoğlu, & E. Aktaş. 2016. Modification of carbon fibre/epoxy composites by polyvinyl alcohol (PVA) based electrospun nanofibres. *Advanced Composites Letters*, **25**, 096369351602500303.
16. Radulescu, D. M., I. A. Neacsu, A. M. Grumezescu, & E. Andronescu. 2022. New insights of scaffolds based on hydrogels in tissue engineering. *Polymers*, **14**, 799.
17. Kesharwani, P., A. Bisht, A. Alexander, V. Dave, & S. Sharma. 2021. Biomedical applications of hydrogels in drug delivery system: An update. *Journal of Drug Delivery Science and Technology*, **66**, 102914.
18. Le, A. T., T. D. H. Le, K. Y. Cheong, & S. Y. Pung. 2022. Immobilization of zinc oxide-based photocatalysts for organic pollutant degradation: A review. *Journal of Environmental Chemical Engineering*, **10**, 108505.
19. Tian, B., & Y. Liu. 2020. Chitosan-based biomaterials: From discovery to food application. *Polymers for Advanced Technologies*, **31**, 2408–2421.
20. Irfan, M., H. Munir, & H. Ismail. 2022. Characterization and fabrication of zinc oxide nanoparticles by gum Acacia modesta through green chemistry and impregnation on surgical sutures to boost up the wound healing process. *International Journal of Biological Macromolecules*, **204**, 466–475.
21. Erol, I., Ö. Hazman, & M. Aksu. 2023. Preparation of novel composites of polyvinyl alcohol containing hesperidin-loaded ZnO nanoparticles and determination of their biological and thermal properties. *Journal of Inorganic and Organometallic Polymers and Materials*, **33**, 731–746.
22. Yang, J. M., J. H. Yang, S. C. Tsou, C. H. Ding, C. C. Hsu, K. C. Yang, C. C. Yang, K. S. Chen, S. W. Chen, and J. S. Wang. 2016. Cell proliferation on PVA/sodium alginate and PVA/poly (γ -glutamic acid) electrospun fiber. *Materials Science and Engineering: C*, **66**, 170–177.
23. Khorasani, M. T., A. Joorabloo, A. Moghaddam, H. Shamsi, and Z. Mansoori Moghadam. 2018. Incorporation of ZnO nanoparticles into heparinised polyvinyl alcohol/chitosan hydrogels for wound dressing application. *International Journal of Biological Macromolecules*, **114**, 1203–1215.
24. Alvandi, H., H. Rajati, T. Naseriye, S. S. Rahmatabadi, L. Hosseinzadeh, and E. Arkan. 2024. Incorporation of Aloe vera and green synthesized ZnO nanoparticles into the chitosan/PVA nanocomposite hydrogel for wound dressing application. *Polymer Bulletin*, **81**(5), 4123–4148.
25. Gholamali, I., and M. Yadollahi. 2020. Doxorubicin-loaded carboxymethyl cellulose/Starch/ZnO nanocomposite hydrogel beads as an anticancer drug carrier agent. *International Journal of Biological Macromolecules*, **160**, 724–735.
26. Yan, E. Y., X. Y. Hao, M. L. Cao, Y. M. Fan, D. Q. Zhang, W. Xie, J. P. Sun, and S. Q. Hou. 2016. Preparation and characterization of carboxymethyl chitosan hydrogel. *Pigment & Resin Technology*, **45**(4), 246–251.
27. Darbasizadeh, B., Y. Fatahi, B. Feyzi-Barnaji, M. Arabi, H. Motasadizadeh, H. Farhadnejad, F. Moraffah, and N. Rabiee. 2019. Crosslinked-polyvinyl alcohol-carboxymethyl cellulose/ZnO nanocomposite fibrous mats containing erythromycin (PVA-CMC/ZnO-EM): Fabrication, characterization and in-vitro release and anti-bacterial properties. *International Journal of Biological Macromolecules*, **141**, 1137–1146.
28. Ban, M. T., N. Mahadin, and K. J. Abd Karim. 2022. Synthesis of hydrogel from sugarcane bagasse extracted cellulose for swelling properties study. *Materials Today: Proceedings*, **50**, 2567–2575.